ELSEVIER

Carbohydrate Polymers 39 (1999) 53–59

Carbohydrate Polymers

Dynamic viscoelasticity and small-angle X-ray scattering studies on the gelation mechanism and network structure of curdlan gels

Toshio Tada[a], Takayoshi Matsumoto[b,*], Toshiro Masuda[c]

[a]Advanced Polymer Laboratory, Minase Research Institute, Sekisui Chemical Co. Ltd., Osaka 618-8589, Japan
[b]Division of Forest and Biomaterials Science, Faculty of Agriculture, Kyoto University, Kyoto 606-8502, Japan
[c]Department of Material Chemistry, Faculty of Engineering, Kyoto University, Kyoto 606-8501, Japan

Received 24 March 1998; received in revised form 27 October 1998; accepted 31 October 1998

Abstract

Small-angle X-ray scattering (SAXS) and dynamic viscoelasticity measurements were carried out to clarify the static network structure of curdlan gels in 0.01 N NaOH at the semi-dilute regime. The structural change during the gelation was also investigated by time resolved measurement with a temperature jump procedure. It was revealed from the time resolved SAXS measurements that the gelation occurred via a structural change from a heterogeneous network structure to a homogeneous network structure. The structural change at the semi-dilute regime would be correlated to the dissociation of the molecular associations, from an associated state to a dissociated state, at the dilute regime. It was also revealed from the results of SAXS measurements that the network structure of curdlan gel is characterized by a mass fractal structure with the fractal dimension of 1.4.

It was clarified by a scaling theory that the curdlan gel consists of a homogeneous network structure. It was shown that the distance between the neighboring cross-linking points could be related to the correlation length determined by the SAXS measurement © 1999 Elsevier Science Ltd. All rights reserved.

Keywords: Curdlan gels; Dynamic viscoelasticity

1. Introduction

Curdlan is an extracellular polysaccharide produced by soil microorganism *Alcaligens faecalis var.* 10C3K (Kanzawa et al., 1987), and its linear structure consists of β-1, 3-glycoside linkages. Sarko et al. clarified by X-ray diffraction measurements that curdlan crystallizes as a triple helix in the solid state (Bluhm and Sarko, 1977; Deslandes et al., 1980). This neutral polysaccharide is not soluble in water but it is soluble in alkaline aqueous solution and polar solvent like dimethyl sulfoxide (Harada et al., 1968; Ogawa et al., 1972). Similar to the other microbial polysaccharide, curdlan and its derivatives has bioactivity such as anti-HIV activity and anti-tumor activity (Hatanaka, 1995; Yoshida et al., 1996; Hotta et al., 1993; Ito et al., 1990). The bioactivity seems to depend on the higher order structure of polysaccharides in solution. The small-angle X-ray scattering (SAXS) measurement is an effective method to characterize the molecular structure of polysaccharide in aqueous systems. Recently, Gawronski et al. studied the dispersed structure of a microbial branched β-1, 3-D-glucan cinerean in aqueous solution (Gawronski et al., 1996a; Gawronski et al., 1996b), and clarified that cinerean dispersed in a rod-like structure in water.

According to our previous investigation about the dispersed structure of curdlan molecules in various concentrations of NaOH at the dilute regime, curdlan molecules associate in lower concentrations of NaOH at 25°C, and they dissociate by heating to 60°C (Tada et al., 1997). The molecular association is characterized as a multi-helical conformation at the higher concentrations of NaOH above 0.05 N (Tada et al., 1998). However, at the lower concentrations of NaOH below O.02 N, the molecular association is characterized as a heterogeneously aggregated coil, which consists of a hydrophilic surface and a hydrophobic core (Tada et al., 1997).

Curdlan gels are easily formed in the concentrated systems and the most of them are thermally irreversible. Kanzawa et al. reported that curdlan gels obtained at 60°C and 90°C show different mechanical properties (Kanzawa et al., 1989a,b). The gel obtained by heating above 60°C is optically transparent, which means that the gel is constructed by a homogeneous network structure. Our previous study showed that the gelation occurred when

---

* Corresponding author. Corresponding address: Division of Forest and Biomaterials Science, Kyoto University, Kyoto 606-8502, Japan.

0144-8617/99/$ - see front matter © 1999 Elsevier Science Ltd. All rights reserved.
PII: S0144-8617(98)00157-X

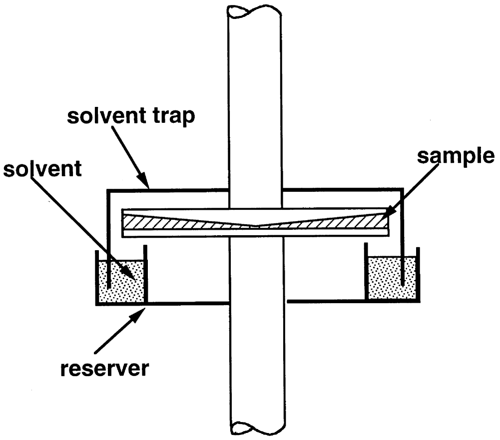

Fig. 1. The devise which prevents samples from drying.

curdlan in lower concentrations of NaOH below 0.05 N is heated above 60°C, and pointed out the gelation mechanism would be correlated to the transition of the molecular association from an associated state to a dissociated state in the dilute regime (Tada et al., 1998).

The SAXS measurement is useful to elucidate the fine structure of not only isolated particles but also the network structure of gels. For instance, Kanaya et al. reported on the phase separation behavior and the network structure of poly (vinylalcohol) gels by small-angle neutron scattering (SANS) (Kanaya et al., 1994), and SAXS measurements (Kanaya et al., 1995), and elucidated that the spinodal decomposition exists during the gelation process. Yuguchi et al. reported on the network structure of gellan gum, a microbial polysaccharide, aqueous systems and determined the cross sectional radius of gyration for the network chain consisting the gel (Yuguchi and Miura, 1996).

The fractal dimension of self similar substances can also be evaluated by the SAXS measurement (Keefer and Schaefer, 1986; Bale and Schmidt, 1984; Höhr et al., 1988), and many kinds of gels seem to be constructed by a fractally rough structure. It is well-known that the fractal structure is constructed by aggregated clusters at the critical point of gelation. Kawai et al. determined the fractal dimension for the gels of sodium alginate aqueous systems (Kawai et al., 1994).

In the present article, we discuss the static structure of curdlan gel and the structural changes during the gelation based on the time resolved SAXS and dynamic viscoelasticity measurements. The static structure of curdlan gel is also discussed in terms of the scaling theory.

2. Experimental

2.1. Sample preparation

The spray-dried powder of curdlan (biochemical grade) was purchased from Wako Pure Chemical Industries, Ltd. (Osaka, Japan). The powder of curdlan was dried in vacuum at room temperature before preparing the alkaline aqueous solutions, and no further purification was carried out. Curdlan solutions in 0.01 N NaOH aqueous solutions were prepared in the N_2 atmosphere to prevent it from being neutralized by CO_2 in the air. All the measurements were carried out against the samples freshly prepared by the above procedure at the room temperature.

2.2. Dynamic viscoelasticity measurements

Dynamic viscoelasticity measurements were carried out by Rheometrics Dynamic Analyzer RDA II (Rheometrics scientific F.E., Tokyo) using the parallel plates or cone-plate geometry with a diameter of 50 mm. The cone angle was 0.04 rad, and the gap used for parallel plates ranged from 0.8 to 1.2 mm. A devise was used to prevent the samples from drying during measurements as shown in Fig. 1. The air-liquid interface of the sample solutions or gels between cone and plate or plates was in saturated pressure of solvent. Temperature was controlled ranging between 30°C and 60°C within 0.5°C by a heater gun equipped in RDA II under flowing of the nitrogen gas. Dynamic strain amplitude at the edge of the parallel plates used in the present study was ranging from 0.0075 to 0.1 where all the samples showed linear viscoelasticity.

2.3. Small-angle X-ray scattering measurements

The SAXS measurement was carried out by the 6 m SAXS camera at High Intensity X-ray Laboratory in Kyoto University. The Ni filtered Cukα line, $\lambda = 1.54$ Å, generated from 3.5 kW rotating anode X-ray generator (RU-1000C3, Rigaku Denki Co. Ltd., Japan) was used for the measurements. Two-dimensional position sensitive proportional counter (256*128 pixels) was used for a detector. The bending mirrors for the point focusing the X-ray were gold coated in order to shorten the accumulation time. The isotropic two-dimensional position of scattering intensity was azimuthally averaged. The scattering intensity of sample solution was corrected by subtracting the intensity of background. The sample-detector length of the present study was about 1.66 m, and temperature control is carried out at the temperature ranging from 25°C to 60°C by a heater with circulation of cold water. The time-resolved measurements were performed to clarify the structural change during the gelation, and the number of photons of scattered X-ray was accumulated every 600 s. The measurements were carried out continuously for six intervals.

3. Results and discussion

3.1. Gelation mechanism and structural changes during gelation for 5 wt.% Curdlan in 0.01 N NaOH aqueous solution

As mentioned in earlier previous article, the molecular

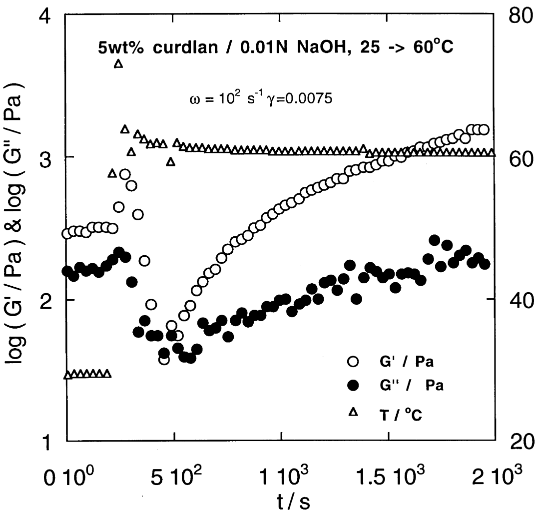

Fig. 2. Temperature jump effect on time dependence of storage G' (open circles) and loss G'' (closed circles) for 5 wt.% curdlan in 0.01 N NaOH aqueous solution. The dynamic strain amplitude γ at the edge is 0.0075 and angular frequency ω is $10^2\ s^{-1}$.

association of curdlan dissociates at 60°C, and gelation occurs in the concentrations of NaOH below 0.05 N. The construction of network structure of the gel would be accompanied with the dissociation. As curdlan is a hydrophobic polymer, the nature of cross-linking points seems to be the hydrophobic interaction (Kanzawa et al., 1987).

Fig. 2 shows the temperature jump (*T*-jump) effect on the time dependence of the storage modulus, G', and loss modulus, G'', at $\omega = 10^2\ s^{-1}$ for 5 wt.% curdlan in 0.01 N NaOH aqueous solution. The *T*-jump from 30°C to 60°C was applied at about $t = 200$ s and the temperature seems to be in an equilibrium at about $t = 300$ s. The time dependence of both the moduli can be divided into four regions as follows: In the first region, just after the *T*-jump ($200\ s < t < 300\ s$), the storage and loss moduli slightly increase. This behavior is originated from the expansion of the molecular association, and the temporal cross-linking points are formed at the boundaries of the molecular associations. In the second region ($300\ s < t < 480\ s$), both the moduli rapidly decrease, which is originated from the dissociation process of the molecular association. Thermal energy of the molecular chains in the molecular association overcomes the hydrophobic interaction, and each molecule becomes diffusive. This results in cleaving the temporal network formed in the first region and decreasing the value of G'. In the third region ($480\ s < t < 1800\ s$), both the moduli slowly increase, which is attributed to the new formation of the intermolecular three-dimensional network. In the fourth region ($t > 1800\ s$), they reach an asymptotic value, in which the system reaches equilibrium condition, and the gelation is completed.

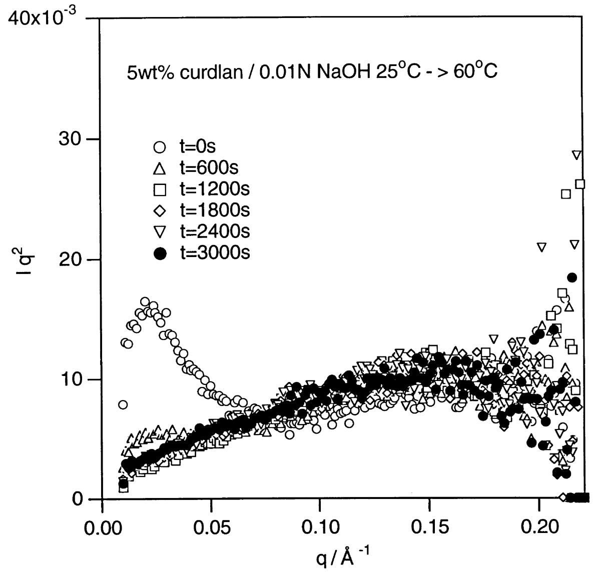

Fig. 3. Temperature jump effect on time dependence of $I(q)q^2$vs.q plot for 5 wt.% curdlan in 0.01 N NaOH aqueous solution.

The structural change during the gelation is also investigated by the time resolved SAXS measurement with the *T*-jump procedure. Fig. 3 shows the Kratky plot ($I(q)\cdot q^2$ vs.q) for 5 wt.% curdlan in 0.01 N NaOH aqueous solution at the intervals of 600 s. Here, $I(q)$ and q respectively represents the scattering intensity and the magnitude of the scattering vector, q, ($q = 4\pi\ \sin(\theta/2)/\lambda$; θ and λ being the scattering angle and the wavelength of an incident X-ray). The *T*-jump from 25°C to 60°C is applied at $t = 0$ s. Dispersive points of the Kratky plot in the value of q larger than 0.18 Å^{-1}was originated from an experimental noise, as the value of $I(q)$ in the large-q is very weak and difficult to detect. Two maximums are observed in the Kratky plot at about $q = 0.15$ Å^{-1} (in large value of q) and $q = 0.02$ Å^{-1} (in the small value of q), just after applying *T*-jump. The structure corresponding to the broad maximum in large-q is smaller in scale than the structure corresponding to that in small-q in the real space. Kanaya et al., reported the similar scattering profile, i.e. two maximums in the Kratky plot become a single maximum with constructing entangled network in the phase separation behavior of poly(vinylalcohol) (PVA) aqueous system (Kanaya et al., 1995).

Two maximums in our data at 25°C suggest that the existence of different network structure in the scale. The maximum in the small-q gradually disappears, and this means that the large structure disappears with time. After 1800 s, there remains only a single maximum at large-q, and the scattering curve is almost invariable beyond this time. It should be noted that this time approximately agrees with the time when the value of G' reaches the equilibrium value, as shown in Fig. 2. The disappearance of the maximum at the small-q seems to accompany with the gelation, and this means that the homogeneous network structures can be characterized by a relatively small structure in scale.

This suggests that there exist a structural change from a heterogeneous structure to a homogeneous network structure in the gelation. The structural change at the semi-dilute

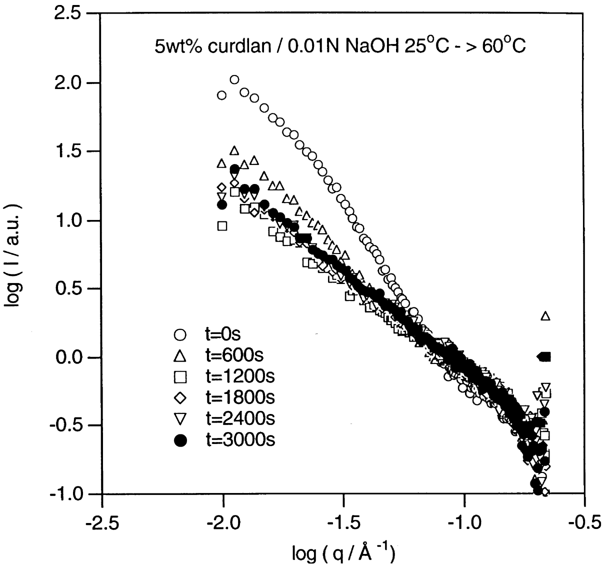

Fig. 4. Temperature jump effect on time dependence of log $I(q)$ vs. log q plot for 5 wt.% curdlan in 0.01 N NaOH aqueous solution.

regime would be associated with the dissociation process of the molecular association at the dilute regime.

Fig. 4 shows the SAXS profile during the gelation from another aspect, where $I(q)$ and q for the same system as Fig. 3 is double logarithmically plotted. Here, an upturn is observed in the SAXS curve at very small values of q for $t = 0$. This upturn is called the Picot–Benoît effect (Bastide, 1996), which is considered to be ascribed to the existence of a long-range correlation in the networks and an interference between scattering objects. Thus the appearance of the Picot–Benoît effect means the network consists of heterogeneous structure. The Picot–Benoît effect disappears with time after 1200 s, which suggests that a large structure in scale disappears. This result agrees with the Kratky plot as shown in Fig. 2.

After 1800 s, the relationship between $I(q)$ and q becomes almost a straight line approximately over a decade, $-2.0 < \log q < -1.0$, and this means that $I(q)$ is expressed by a single exponential function of q. The absolute value of the exponent, α, gives a fractal dimension of a substances as expressed by the following equation (Ogawa, 1990):

$$I(q) \sim q^{-\alpha}. \quad (1)$$

Here, the fractal structure is divided into the surface fractal ($\alpha = 2d\text{-}D$) and the mass fractal ($\alpha = D$) in the d-dimensional space. We can distinguish them easily from the value of the exponent i.e. $1 < \alpha < 3$ for mass fractal and $3 < \alpha < 4$ for surface fractal, respectively in the three-dimensional space (Bastide and Candau, 1996). As the value of α in the present study is approximately estimated to be 1.4, the mass fractal structure seems to be constructed with the gelation. The construction of fractal structure suggests that the gel consists of the homogeneous structure in macroscopic sense.

Kawai et al. evaluated the fractal dimension for the gel of α-L-guluronic acid-rich sodium alginate acids in $MgCl_2$ aqueous solution to be 1.45 (Kawai et al., 1994), and this value is very similar to the value obtained in the present study. It should be noted that the time for constructing the fractal structure agrees with the time when the maximum is small q region in the Kratky plot disappears. This means that the formation of the fractal structure accompanies with the structural change from the heterogeneous to homogeneous structure. Based on the fact that the heterogeneous molecular association dissociates at 60°C, the heterogeneous structure before gelation consists of both the long-range and short range correlation lengths, and the homogeneous structure after gelation consists of single correlation length.

The fractal dimension is useful to discuss the static structure of gels. The value of α is connected with the exponent v which represents the degree of expansion for a molecular chain as follows:

$$\alpha v = 1. \quad (2)$$

Also the exponent v is correlated to the end to end distance R as follows:

$$R \sim bN^{v}. \quad (3)$$

Here, b and N denote the unit segment length and the number of the segment in a polymer chain, and the value of v is expected to be 1/2 and 3/5 for the Gaussian chain and the polymers in a good solvent, respectively. Schaefer et al. reported for the polystyrene in cyclopentane system that the value of α is 2 at the Θ temperature, and this value gradually approaches to 5/3 with increasing temperature (Miyaji and Ogawa, 1989). Thus, the value of α is expected to be 1.67 for the polymers in a good solvent, and our values of α for curdlan gel would not be so far from 1.67. This suggests that the networks of curdlan gel would be similar to the state of the polymers in a good solvent. This point will be discussed in Section 3 by using a scaling theory.

As shown in Fig. 4, all of the SAXS profiles vary approximately proportional to q^{-4}in large-q ($\log q > -0.75$), that is, the Porod region. The appearances of the Porod means that the electric density of scattering objects has a clear boundary in sufficiently small length scale.

3.2. Network structure of Curdlan gel

The equilibrium structure of curdlan gel was studied using the scaling theory of des Cloizaux for the various concentrations of curdlan in 0.01 N NaOH aqueous solution. This scaling theory for polymers at the semi-dilute regime predicts the relationships between the osmotic pressure, Π, the correlation length, ξ, the polymer volume fraction, ϕ, and the osmotic bulk modulus, K_{os}, as follows (Bastide and Candau, 1996):

$$\Pi \sim \xi^{-3} \sim \phi^{s} \sim K_{os}. \quad (4)$$

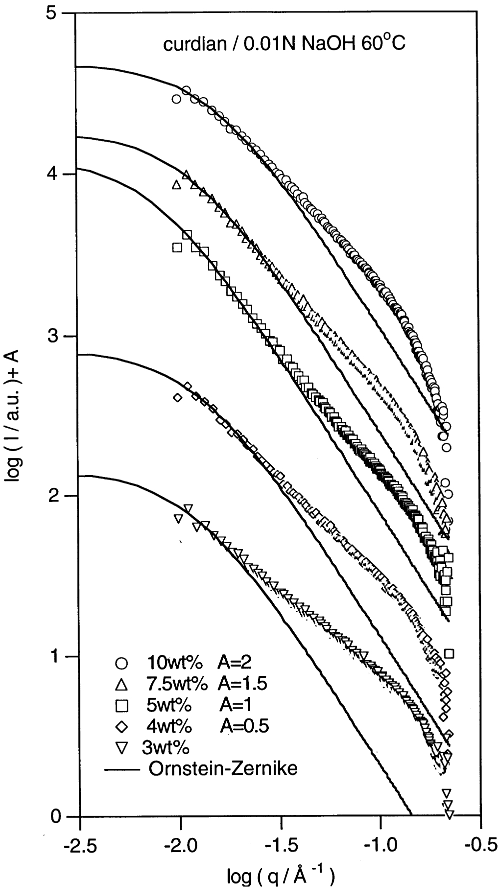

Fig. 5. Double logarithmic plot between $I(q)$ and q plot for various concentrations of curdlan in 0.01 N NaOH aqueous solution at 60°C. Solid lines denote the least square fitting curves of Ornstein Zernike equation.

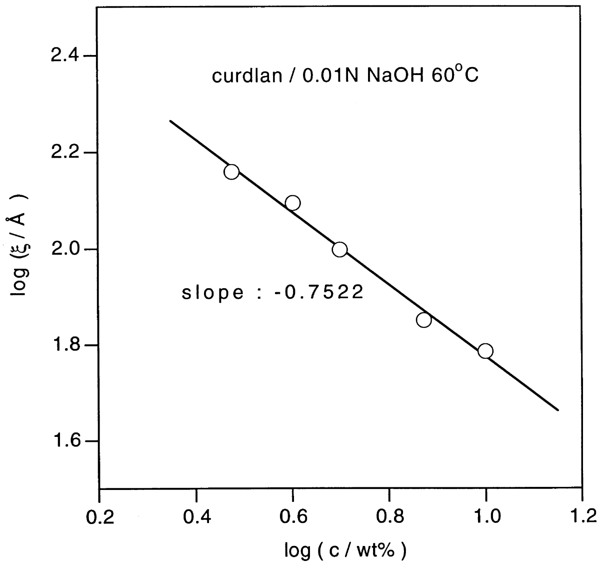

Fig. 6. Correlation length ξ is double logarithmically plotted against concentration of curdlan in 0.01 N NaOH aqueous solution at 60°C.

Here, the exponent s can be connected with ν as $s = 3d\nu/(3d\nu\text{-}1)$ for the d-dimensional space, and the value of s is expected to be 2.25 for the polymers in a good solvent ($\nu = 3/5$). According to de Gennes, the term ‘‘semi-dilute regime’’ means that the volume fraction of polymer is much larger than the overlapping volume fraction of the polymer chain, ϕ^*, while much smaller than that of the polymer matrix,

$$\phi^* \ll \phi \ll 1.$$

As Eq.(4) is derived from the c* theory, or mean field theory, this scaling law fails in explaining the heterogeneous networks and the local structure. In the case of the three-dimensional space, the relationship between the correlation length and the polymer volume fraction for polymer in a good solvent is calculated from Eq. (4) as follows:

$$\xi \sim \phi^{-3/4}. \tag{5}$$

The correlation length can be determined from the SAXS measurement by using the Lorentzian type Ornstein–Zernike equation as shown in Eq. (5) (Bastide and Candau, 1996; Berne and Pecora, 1990).

$$I(q)) = I(0)/(1 + q^2\xi^2). \tag{6}$$

Here $I(0)$ denotes the zero angle scattering intensity.

The values of $I(q)$ for the various concentration of curdlan in 0.01 N NaOH aqueous gels at 60°C are double logarithmically plotted against q in Fig. 5. Each SAXS curve is vertically shifted by a shift factor A to avoid overlapping them, except for 3 wt.%. We can estimate the value of correlation length by the least-squares fitting of Eq. (6) as shown by the solid lines in Fig. 5. For heterogeneous network systems, the correlation length must be calculated by the squared-Lorentz type Ornstein–Zernike equation that is derived from the Debye–Bueche equation (Koberstein et al., 1985). The values of correlation length estimated from both the equations are approximately the same value. Moreover, the Picot–Benoît effect cannot be seen in the scattering profiles at 60°C, we used the value of correlation length estimated from the line shape Lorentzian equation for simplicity. In general, this approximation is valid.

In Fig. 6, the correlation length is double logarithmically plotted against concentration of curdlan 60°C. The relationship can be approximated by a straight line with a slope of $-$ 0.752, and the experimental results agree with the theoretical prediction from Eq. (5) under an assumption that the relation between the volume fraction and the weight concentration of polymer solution, c, can be written as $c \approx 100{\cdot}\phi$. This relationship suggests that the network in the gel is constructed by the homogeneous structure. We can treat the network structure of gel as that of the polymer chains in a good solvent at the semi-dilute regime.

The scaling theory for the polymer in a good solvent at the semi-dilute regime is extended to the swelling gel in a

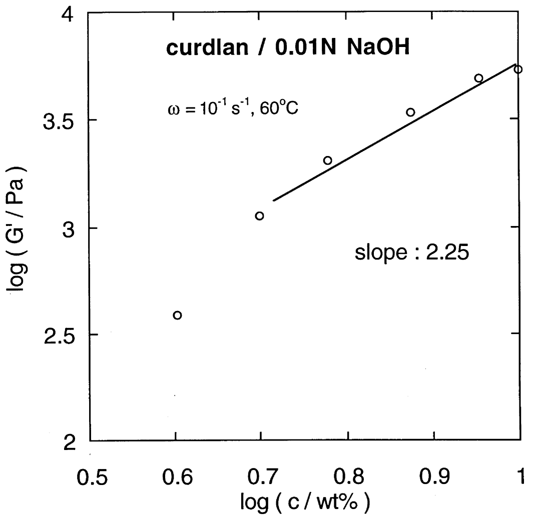

Fig. 7. Storage modulus G' at $\omega = 10^{-1}$ s^{-1} is double logarithmically plotted against concentration of curdlan in 0.01 N NaOH aqueous solution at 60°C.

good solvent as following equation (Bastide and Candau, 1996; Horkay, 1989).

$$G(\phi_e) \sim \phi_e^{\nu d/(\nu d-1)}. \quad (7)$$

Here, ϕ_e and G are the polymer volume fraction in the gel at the maximum swelling and the shear modulus of the gel, respectively. In the three-dimensional space, the exponent of ϕ_e is expected to be 2.25 in the concentrations of polymer sufficiently higher than the gelation point. It should be noted that the value of exponent for a swelling gel is the same value as the value of the polymer in a good solvent.

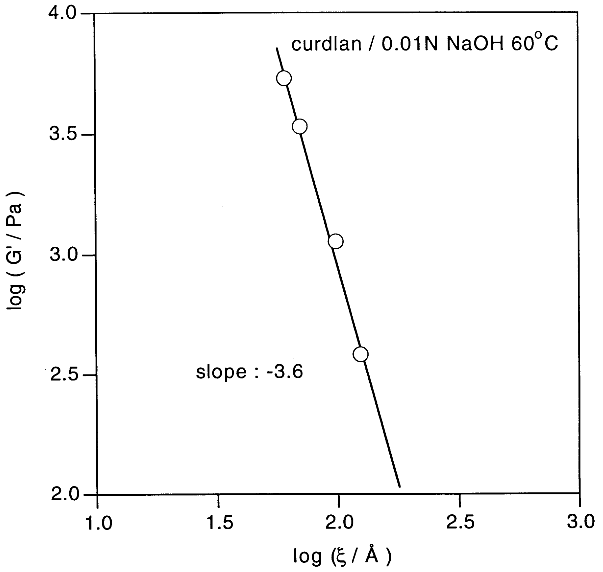

Fig. 8. Storage modulus G' at $\omega = 10^{-1}$ s^{-1}double logarithmically plotted against the correlation length ξ for various concentrations of curdlan in 0.01 N NaOH aqueous solution at 60°C.

In Fig. 7, the value of G′ in the plateau region ($\omega = 0.1\ s^{-1}$) are plotted double logarithmically against the concentrations of curdlan at 60°C. The relationship is approximately fitted by a straight line with slope of 2.25. However, the slope seems to increase as the concentrations of curdlan below 5 wt.%. This suggests that the threshold of gelation seems not so far from 5 wt.%, and Eq. (7) is invalid for the region near the gelation point.

In order to connect the results obtained from the SAXS measurements with these obtained from the dynamic viscoelastic measurements, we use a new equation by connecting the equation for the swelling gel in a good solvent with that for the polymer in good solvent as follows:

$$G(\phi_e) \sim \xi(\phi_e)^{-3}. \quad (8)$$

Fig. 8 shows the double logarithmic plot between the value of G′ in the plateau region and the correlation length for various concentrations of curdlan in 0.01 N NaOH aqueous solution at 60°C. As shown in Eq. (8), the exponent of the correlation length is expected to be − 3. However, as shown in Fig. 8, the absolute value of the exponent seems to be slightly larger than 3. Considering the polydispersity of the natural polysaccharide, this result is not so far from the theoretical prediction. According to the rubber elasticity theory, the plateau modulus can be estimated from the number cross-linking density, which can be estimated from the correlation length for the appropriate lattice. The calculated values of the plateau modulus approximately agree with the experimental values within the error of 0.35% on the assumption that the unit cell of the network chain is the face-centered lattice. This implies that the relationship between structural information obtained by the SAXS measurements and mechanical information obtained from the dynamic viscoelasticity measurements seems to be expressed by the simple scaling theory. This result implies that the obtained value of correlation length is related to the mechanical point which is an origin of elasticity, that is, the correlation length seems to correspond to the distance between the cross-linking points. The networks of curdlan gel are characterized by blobs whose diameter is correlation length.

4. Conclusion

It was clarified from the results of the time resolved dynamic viscoelasticity and SAXS measurements that the gelation of curdlan occurred via the structural change from a heterogeneous structure to a homogeneous structure, and each structure corresponds to the associated state and dissociated state of the molecular association at the dilute regime. According to the scaling theory, a good agreement can be seen in the relationship between the results of dynamic viscoelasticity and SAXS measurements. Also the growth of the fractal structure during the gelation process is kinetically investigate by time resolved SAXS measurements.

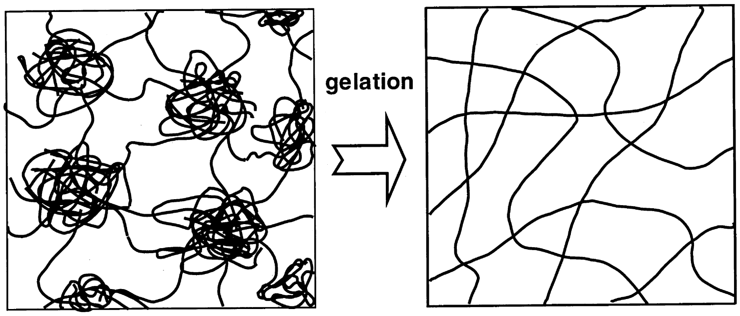

Fig. 9. Models for the transition from inhomogeneous to homogeneous network structure. Left panel and right panel represent the heterogeneous structure and homogeneous structure, respectively.

The fractal structure of gel is characterized by the mass fractal of dimension about 1.4. The gelation process is schematically illustrated as Fig. 9, in which the heterogeneous network at 25°C becomes homogeneous network by dissociation, and after dissociation process, mass fractal structure is constructed.

References

Bale, H. D., & Schmidt, P. W. (1984). Small-angle X-ray scattering investigation of submicroscopic porosity with fractal properties. *Phys. Rev. Letts.*, *53*, 596–599.

Bastide, H.J., & Candau, S.J. (1996). *The physical properties of polymeric gels* (pp. 157–168). New York: Wiley.

Berne, B.J., & Pecora, R. (1990). In: E. Robert (Ed.), Dynamic light scattering (pp. 257–261). Malabar, Florida: Kliefer Publishing Co.

Bluhm, T. L., & Sarko, A. (1977). The triple helical structure of lentinan, a linear (1 → 3)-β-D-Glucan. *Can. J. Chem.*, *55*, 293–303.

Deslandes, Y., Marchessault, R. H., & Sarko, A (1980). Triple helical structure of (1 → 3)-β-D-Glucan. *Macromolecules*, *13*, 1466–1471.

Gawronski, M., Aguirre, G., Conrad, H., Springer, T., & Stahmann, K.-P. (1996). Molecular structure and precipitates of a rodlike polysaccharides in aqueous solution by SAXS experiments. *Macromolecules*, *29*, 1516–1520.

Gawronski, M., Conrad, H., Springer, T., & Stahmann, K.-P. (1996). Conformational changes of the polysaccharide cinerean in different solvents from scattering methods. *Macromolecules*, *29*, 7820–7825.

Hatanaka, K. (1995). Perspectives of glycotechnology. *High Polymers Japan*, *44*, 558–560.

Harada, T., Misaki, A., & Saito, H. (1968). Curdlan: bacterial gel-forming β-1,3-glucan. *Archiv. Biochem. Biophys.*, *124*, 292–298.

Höhr, A., Neumann, H.-B., Schmidt, P. W., Pfeifer, P., & Avnir, D. (1988). Fractal surface and cluster structure of controlled-pore glasses and Vycor porous glass as revealed by small-angle X-ray and neutron scattering. *Phys. Rev. B*, *38*, 1462–1467.

Horkay, F., Hecht, A. M., & Geisslar, E. J. (1989). The effects of crosslinking on the equation of sate of a polymer solution. *Phys. Chem*, *91*, 2706–2711.

Hotta, H., Hagiwara, K., Kimura, S., & Hirata, A. (1993). Augmentation of protective immune responses against sendai virus infection by fungal polysaccharide schizophyllan. *Int. J. Immunopharmac.*, *15*, 55–60.

Ito, W., Sugawara, K., Kimura, S., Tabata, K., Hirata, A., Kojima, T., Mori, S., & Shimada, K. (1990). Immunopharmacological study of sulfated schizophyllan (SPG)I – its action as a mitogen and Ant-HIV agent. *Int. J. Immunopharmac.*, *12*, 225–233.

Kanaya, T., Ohkura, M., Kaji, K., Furusawa, M., & Misawa, M. (1990). Structure of poly(vinyl alcohol) gels studied by wide and small-angle neutron scattering. *Macromolecules*, *27*, 5609–5615.

Kanaya, T., Ohkura, M., Takeshita, H., Kaji, K., Furusawa, M., & Yamaoka, H. (1995). Gelation process of poly(vinyl alcohol) as studied by small-angle neutron and light scattering. *Macromolecules*, *28*, 3168–3174.

Kanzawa, Y., Harada, T., Koreeda, A., & Harada, A. (1987). Curdlan gel formed by neutralizing its alkaline solution. *Agric. Biol. Chem.*, *51*, 1839–1843.

Kanzawa, Y., Koreeda, T., Harada, A., & Harada, T. (1989a). Electron microscopy of the gel forming ability of polysaccharide food additives. *Agric. Biol. Chem.*, *53*, 979–986.

Kanzawa, Y., Koreeda, T., Harada, A., & Harada, T. (1989b). Difference of molecular association in two types of curdlan gel. *Carbhydr. Polym.*, *10*, 299.

Kawai, M., Matsumoto, T., & Masuda, T. (1994). Rheological properties of gel of alginic acid. *T. J. Chem. Soc. Jpn.*, *2*, 108–114.

Keefer, K. D., & Schaefer, D. W. (1986). Growth of fractally rough colloids. *Phys. Rev. Lett.*, *56*, 2376–2379.

Koberstein, J. T., Picot, C., & Benoît, H. (1985). Light and neutron scattering studies of excess low-angle scattering in moderately concentrated polystyrene solutions. *Polymer*, *26*, 673–681.

Miyaji, H., & Ogawa, T. (1989). Fractals in polymers. *High Polymers, Japan*, *38*, 50–63.

Ogawa, K., Turugi, J., & Wantnabe, J. (1972). Conformational behavior of a gelforming (1 → 3)-β-D-glucan in alkaline solution. *Carbohydr. Res.*, *29*, 399–405.

Tada, T., Matsumoto, T., & Masuda, T. (1997). Influence of alkaline concentration on molecular association structure and viscoelastic properties of curdlan aqueous systems. *Biopolymers*, *42*, 479–487.

Tada, T., Matsumoto, T., & Masuda, T. (1998). Structure of molecular association of curdlan at dilute regime in alkaline aqueous systems. *Chem. Phys.*, *128*, 155.

Yoshida, T., Hattori, K., Sawada, Y., Choi, Y., & Uryu, T. (1996). Graft copolymerization of methyl methacrylate onto curdlan. *J. Polym. Sci. Polym. Chem.*, *34*, 3053–3060.

Yuguchi, Y., Miura, M., Urakawa, H., Kitayama, S., Ohno, S., & Kajiwara, K. (1996). Small-angle X-ray characterization of gellan gum containing a high content of sodium in aqueous solution. *Carbohydrate Polymers*, *30*, 83–94.

Ogawa, T. (1990). Small-angle X-ray scattering from the surfaces of polymer crystals. *J. Phys. Soc. Jpn*, *59*, 3642–3649.